COMPUTATIONAL BEAM DYNAMICS STUDIES FOR IMPROVING THE RING INJECTION AND EXTRACTION SYSTEMS IN SNS*

J.A. Holmes, S. Cousineau, M.A. Plum, J.G. Wang, ORNL, Oak Ridge, TN 37830, U.S.A.

Abstract

The ring injection and extraction systems must function as designed in order for the Spallation Neutron Source (SNS) to achieve its specified performance. In commissioning and early operations we have encountered problems that have been traced to these systems. We experienced high beam losses in and around the injection dump, the rectification of which has necessitated ongoing study and development by a multidisciplinary team. Results already include a number of enhancements of existing features and the addition of new elements and diagnostics. The problem in the extraction region stems from tilted beam distributions observed in the ring-to-target beam transport line (RTBT) and on the target, thus complicating the control of the beam-on-target distribution. This indicates the inadvertent introduction of x-y beam coupling somewhere upstream of the RTBT. The present paper describes computational studies, using the ORBIT Code, addressed at the detailed understanding and solution of these problems.

INJECTION ISSUES

To reach its specified operating parameters, SNS must achieve the unprecedented low uncontrolled losses of one part in 10^4. Thus far, the most severe losses are observed in the vicinity of the ring injection. The SNS ring injection system (Fig. 1) utilizes a stripper foil to convert a 1 GeV H^- linac beam to a circulating H^+ beam in the accumulator ring [1]. The injection dump was designed [2] to collect H^- beam that misses the stripper foil and also incompletely stripped H^0 beam. The injection system is rather complicated because it is necessary to simultaneously satisfy several constraints, which are described in detail in Ref. [3]. The simultaneous satisfaction of all these constraints is difficult and, indeed, was not even possible in the injection system as originally constructed.

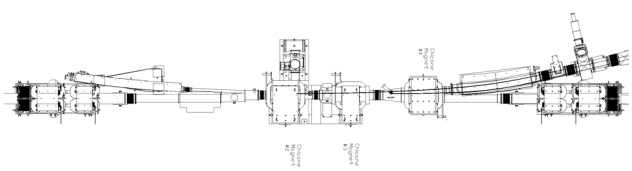

Figure 1: SNS ring injection area.

Due to unacceptable beam losses in the injection dump region, detailed experimental and computational studies of the SNS injection system were undertaken [3-5] along with a program to fix the problem. Based on the results of these studies, a number of mitigating actions were taken. The second stripper foil was widened to better intercept both the H^- and H^0 waste beam components, which were further separated than was originally thought. The chicane and septum magnet settings and the primary stripper foil position were changed from the original design values to optimize the injection process. The fourth injection chicane magnet was moved to bring the H^- waste beam component into the good field region and thereby correct its unwanted vertical displacement. A C-magnet was installed after the injection dump septum to provide independent steering of the H^- and H^0 waste beam components. The dump septum magnet was significantly modified to provide greater aperture for the waste beams. Finally, additional diagnostics (BPMs, wire scanners, and a view screen) were added to the dump line to allow for precise characterization of the waste beams. While much improvement was gained through these modifications, there are outstanding issues and further enhancements may be necessary.

A Second Quadrupole

One such issue involves whether there is adequate control of the two waste beam components in the injection dump line. This line is more than 26 m in length from the downstream end of the dump septum magnet to the dump itself. The intervening space contains just the C-magnet, shortly beyond the septum, and a defocusing quadrupole, about 6 m past the septum. This system provides no independent control of the horizontal and vertical beam focusing. In order to do so, we have studied the impact of adding a second quadrupole magnet downstream of the existing quadrupole in order to create a doublet configuration. Three possible locations for the second magnet were considered: L = 1.0 m, 2.5 m and 5.0 m downstream of the existing quadrupole. Because the aperture of the dump line is circular and the horizontal and vertical emittances of the two waste beam components are comparable, we set as a requirement that the horizontal and vertical beta functions be of similar value at the dump. Operational requirements on beam losses and on maximum current density at the dump constrain 1000 m $< \beta_{x,y} <$ 6000 m. Both optics studies using MAD [6] and tracking with ORBIT [7] were carried out starting at the exit of the dump septum. The initial Twiss parameters for the optics studies were taken from independent MAD calculations of the separate H^- and H^0 waste beam components from the point of injection at the primary stripper foil through the dump septum. These were nearly equal, and were also in reasonable agreement with statistical values of the lattice functions calculated using ORBIT's 3D field tracker through the same

* ORNL/SNS is managed by UT-Battelle, LLC, for the U.S. Department of Energy under contract DE-AC05-00OR22725.

elements, with the 3D fields calculated using OPERA-3D/TOSCA [8]. The initial beams used in the dump line tracking studies were taken from the output of these same 3D tracking calculations.

When optics and tracking studies were performed using two quadrupoles, we found that the L = 1.0 m separation is preferable to the 2.5 m and 5.0 m separations. We observed a greater range of quadrupole strengths consistent with target beam size requirements for 1.0 m. Also, the maximum horizontal excursions of the waste beams from the beam pipe center (due to the first defocusing quadrupole) were smaller at 1.0 m separation. Accordingly, we focus on the 1.0 m separation. The MAD calculations for the dump lattice with an additional quadrupole gave acceptable solutions with $\beta_x = \beta_y$ for a wide range of upstream defocusing quadrupole strengths k1 = (-0.70 → -0.0) m^{-2}. The strengths of the downstream quadrupole fall in the range k = (-0.70→ 0.60) m^{-2}. Thus, the downstream quadrupole may be focusing or defocusing, depending on the upstream quadrupole setting. For the single quadrupole lattice, $\beta_x = \beta_y$ only at one setting, k1 = -0.56. However, both β_x and β_y fall in the acceptable range when kl = (-0.65 → -0.39 m^{-2}. A strategy for using the downstream quadrupole could be to set the upstream quadrupole in this single magnet range and then use a weak setting downstream to optimize the focusing.

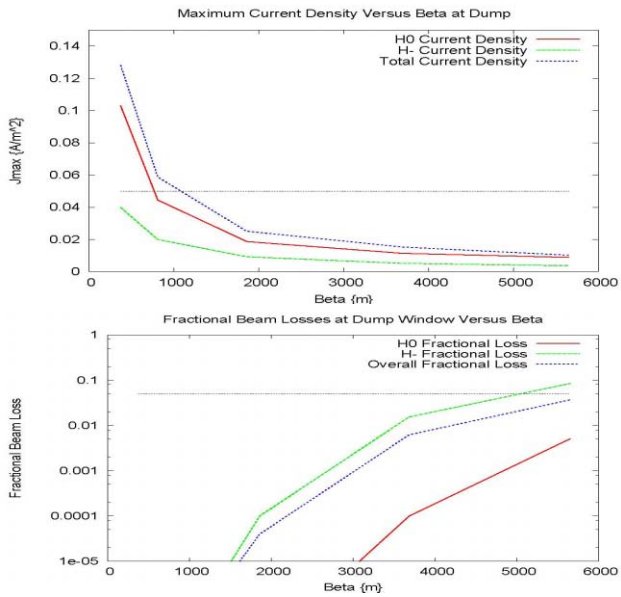

Figure 2: Maximum current density and fractional beam loss versus β at the target. Horizontal lines denote the operational limits.

To illustrate the flexibility gained through the addition of a quadrupole, we carried out ORBIT tracking simulations in the dump line for the L = 1.0 m separation doublet for several settings chosen to give a range of $\beta_x = \beta_y$ at the dump. The initial distributions were taken from 3D tracking simulations of the H^- and H^0 beam components from the stripping foil through the dump septum. Figure 2 shows the maximum current density and fractional beam losses for the H^-, H^0, and overall beam components. For $\beta_{x,y} < 1000$ m, the peak current density at the dump window exceeds specifications, while losses are greater than allowed when $\beta_{x,y} > 6000$ m.

Although a second quadrupole would provide additional flexibility, the present one-quadrupole solution yields a range of settings where the horizontal and vertical beam sizes fall within the constraints.

Losses and Foil Scattering

Even though beam losses have been significantly reduced by the measures described above, the injection region continues to be one of the highest loss regions in SNS. With present beam intensities exceeding 0.5 MW and increasing, there is much effort to understand the cause of the losses. One contributing factor is scattering from the primary and secondary stripper foils. Previous estimates of fractional losses from scattering in the primary foil (~0.3 mg/cm^2 carbon) are in the 10^{-6} - 10^{-5} range, assuming about 7 foil hits for each injected proton, on average. The secondary foil is much thicker than the primary foil (~18 mg/cm^2 carbon), and scattering of the waste beam components could contribute to losses. Studies have been carried out of beam loss increases when the secondary stripper foil is replaced by the secondary foil viewscreen, which consists of 1 mm AL_2O_3. We have modeled the scattering by the secondary stripper foil and also by the secondary foil viewscreen using ORBIT's foil and collimation model, which includes multiple Coulomb scattering, Rutherford scattering, and nuclear elastic and inelastic scattering. To obtain reasonable statistics, 10^6 particles were used in the scattering calculations.

Figure 3 shows the number of particles with scattering angle exceeding the indicated value for the secondary viewscreen. The top figure shows small angle scattering (< 5 mr). In this regime, the ORBIT results agree very well with the multiple Coulomb scattering formulation in Jackson [9]. The middle figure shows the transition from multiple Coulomb to Rutherford scattering in the range from 4 → 10 mr. The bottom figure shows the scattering at large angles. The difference between the ORBIT and Rutherford scattering results is due to nuclear elastic scattering. ORBIT also takes account of inelastic nuclear scattering by removing inelastic scattered particles from the beam. For the secondary viewscreen, the ORBIT calculation yields 2485 particles, about 0.25% of the beam, to inelastic scattering. The results are similar for the secondary foil: multiple Coulomb scattering is appropriate inside 0.7 mr, the transition to Rutherford scattering occurs between 0.7 → 0.8 mr, Rutherford scattering is dominant between 0.8 → 5.0 mr, and nuclear elastic scattering dominates at larger angles. For the secondary foil, 119 particles, about 0.01% of the beam, undergo inelastic scattering.

Finally, we transported H^- and H^0 beam distributions from the injection point (primary stripper foil) to the injection dump for three scenarios: no secondary foil scattering, secondary foil scattering, and secondary viewscreen scattering. With no scattering, 0.3% of the waste beams were lost before reaching the injection dump. With the secondary foil scattering, 0.6% was lost,

and with the viewscreen, 25.6% is lost. Thus, foil scattering contributes to the observed losses to at least some extent, and a thinner secondary stripper foil should improve the situation.

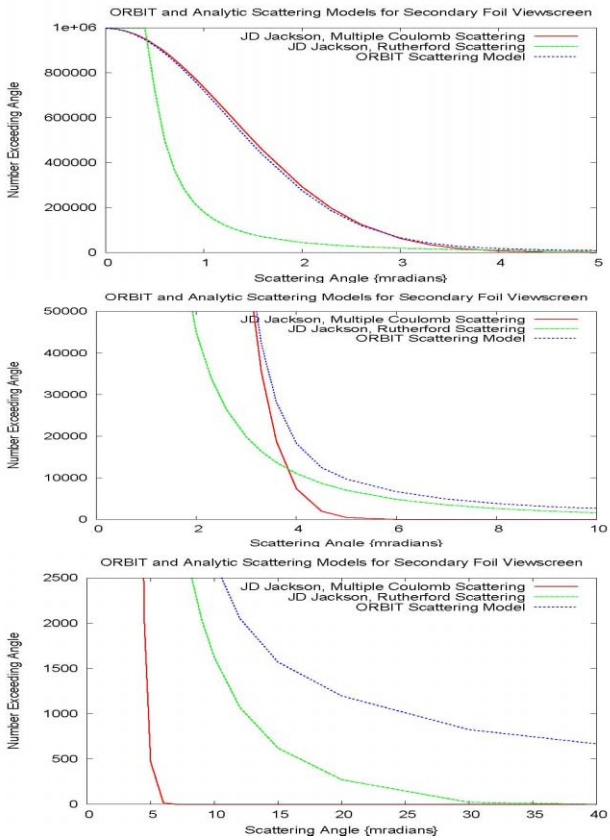

Figure 3: Distribution of scattering angles due to the secondary foil viewscreen.

X-Y COUPLING IN THE RTBT

The RTBT is the transport line from the accumulator ring to the mercury target in SNS. Following the extraction septum, the RTBT is about 150 m long and contains 30 quadrupole magnets and a bend to accommodate the extraction dump. During operation the beam image at the target is observed to be rotated in the x-y plane by as much as 7°, and other observations using wire scanners and BPMs throughout the RTBT show significant beam tilting. These observations indicate that x-y coupling is introduced somewhere upstream. Although some x-y coupling does occur in the ring due to the off-center passage of the beam through the injection chicane bends, tracking calculations have shown that the observed beam tilting in the RTBT is due primarily to the skew quadrupole moment in the extraction septum magnet, which was calculated using OPERA-3D/TOSCA.

Correction of the observed x-y coupling is under consideration. One method is through the introduction of skew quadrupoles in the RTBT shortly downstream of the extraction septum. We have carried out ORBIT tracking studies using up to four skew quadrupoles, and have found that two skew quadrupoles are sufficient to remove the beam tilting throughout the RTBT. The required focusing strengths are fairly small at $k1s < 0.1\ m^{-2}$. Figure 4 shows beam footprints at the target window calculated both without and with x-y coupling correction.

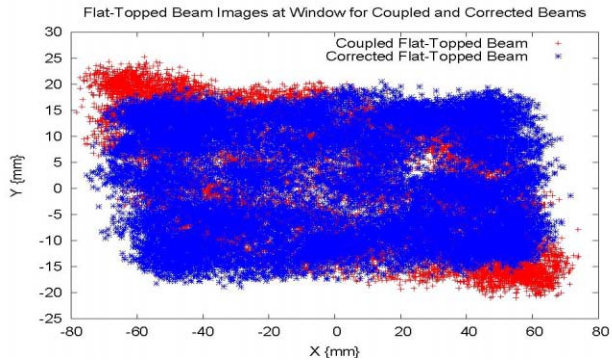

Figure 4: Beam footprints at the target window without (red) and with (blue) correction of the x-y coupling.

CONCLUSIONS

Computational beam dynamics continues to provide guidance in the analysis, understanding, and resolution of issues critical to the successful operation of SNS. We have presented here examples of the use of computational methods to understand and improve losses in the injection region and x-y coupling in the RTBT.

REFERENCES

[1] J. Wei, "Preliminary Change Request for the SNS 1.3 GeV-Compatible Ring", BNL/SNS Tech. Note 76, May, 2000.

[2] D. Raparia, Y.Y. Lee, J. Wei, and S. Henderson, "Beam Dump Optics for the Spallation Neutron Source," PAC'03, Portland, May 2003, FPAB064; http://cern.ch/AccelConf/p03/PAPERS/FPAB064.PDF.

[3] J. A. Holmes, M.A. Plum, J.G. Wang, Y. Zhang, and M. Perkett, "ORBIT Injection Dump Simulations of the H^0 and H^- Beams," PAC'07, Albuquerque, June 2007, THPAS076; http://cern.ch/AccelConf/p07/PAPERS/THPAS076.PDF.

[4] J. G. Wang, "3D Modeling of SNS Ring Injection Dump Beam Line," PAC'07, Albuquerque, June 2007, THPAS078; http://cern.ch/AccelConf/p07/PAPERS/THPAS078.PDF.

[5] J. G. Wang and M.A. Plum, Phys. Rev. ST Accel.Beams 11, 014002 (2008).

[6] H. Grote and F. Christoph Iselin, The Mad Program, Version 8.19, User's Reference Manual, CERN/SL/90-13, (Geneva, 1996).

[7] J.A. Holmes, S. Cousineau, V.V. Danilov, S. Henderson, A. Shishlo, Y. Sato, W. Chou, L. Michelotti, and F. Ostiguy, *in The ICFA Beam Dynamics Newsletter*, Vol. 30, 2003.

[8] Vector Fields: Software for Electromagnetic Design, "TOSCA", Cobham Group Company, 2005, http://www.vectorfields.com/content/view/27/5

[9] J.D. Jackson, "Classical Electrodynamics," Wiley, (New York: 1967).